Supplementary Figures and Figure Legends.

Supplementary Fig. 1. Related to Fig. 1A, B. A. Bar graphs depicting the percentage of ER positive HER-2 negative metastatic breast cancer patients at MD Anderson Cancer Center who were treated with each of the three different CDK4/6 inhibitors (i.e., palbociclib, ribociclib and abemaciclib) from January 2015-February 2023, separated into three-time intervals (T1: January 2015-December 2020; T2: January 2021-December 2021; T3 January 2022 to February 2023). The number of patients treated with each CDK4/6 inhibitor is included in the table below the bar graphs. **B,** Top Schematic representation of the generation of T47D PR (T-PR) cells, which were generated as described in Fig. 1A over a 6.5-month period. Representative bright-field images from each T-PR cell line are shown at 10× magnification. Four cell lines resistant to palbociclib (1.2T-PR, 2.4T-PR, 3.6T-PR, and 4.8T-PR) were generated corresponding to cells resistant to respective concentrations of palbociclib. Bottom left: Dose-response curves for T47D parental (Par) and T-PR cells, determined as described in Fig. 1A. The dashed line indicates IC_{50} values. Bottom right graphs: Horizontal bar graphs showing IC_{50} values and doubling times, determined as described in Fig. 1A. **C–E,** Bar graphs indicating the percentage of cells in S phase by cell line and CDK4/6i. In each graph, the first bar represents parental cells, the next four bars represent parental cells after palbociclib or abemaciclib treatment, and the last four bars represent resistant cell lines. **F** and **G,** 5-Ethynyl-2´-deoxyuridine (EdU) incorporation in parental vs resistant cell lines treated with the indicated concentrations of palbociclib or abemaciclib. For all panels, graphs depict the mean ± SEM; $n \geq 3$ independent experiments. For **C–G**, the differences between parental cells vs the indicated groups were evaluated by one-way ANOVA, Dunnett multiple comparisons test. ** $P < 0.001$; **** $P < 0.0001$; ns: not significant.

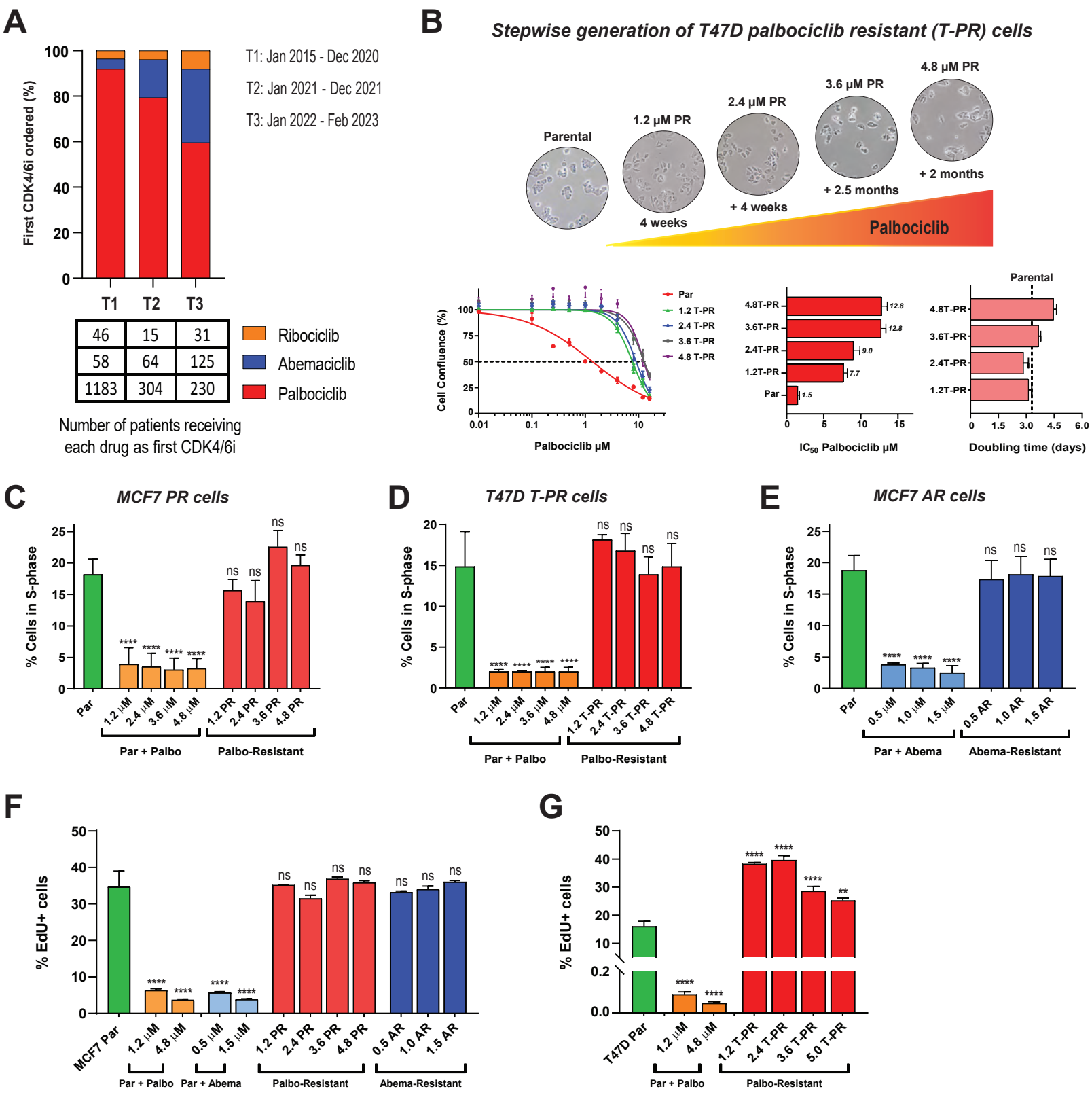

Supplementary Figure 1. Related to Figure 1A - B

Supplementary Fig. 2. Related to Fig. 1A–E. A, Schematic representation of experimental design to test whether long-term culture in drug-free medium resensitizes resistant cells to palbociclib. The resistant cell line panels were cultured in the presence (+D) or absence of palbociclib for 1 week (−D 1w) or 3 weeks (−D 3w) and then treated with increasing concentrations (0.01–16 μM) of palbociclib for 6 days, followed by 6 days of recovery in drug-free medium. **B** and **C,** Dose-response analysis for each PR cell line cultured and treated as described in **A** Cell confluence (whole well) was assessed using Incucyte. Data were normalized to DMSO (100%), and dose-response curves were plotted and analyzed by nonlinear regression using GraphPad Prism 9 software. The dashed lines indicate IC_{50} values. Each experiment included eight technical replicates per concentration and was repeated at least three times. **D,** Cell cycle analysis comparing the effect of palbociclib treatment on T47D parental cells (first five bars) vs PR cell lines in the continuous presence of the drug (+D, middle four bars) and after 1 week of drug removal (−D, last four bars). Stacked bars represent the percentage of cells in each cell cycle phase, by color. **E,** Western blot analysis with the indicated antibodies in T47D parental and PR cells under the conditions described in **D**. **F,** Top: Schematic representation of experimental design to test whether long-term culture in drug-free medium resensitizes resistant cells to abemaciclib. The culture conditions and treatment were as described in **A**, with abemaciclib instead of palbociclib. Bottom: Dose-response analysis conducted as described for **B** and **C.** For all panels data represent the mean ± SEM; $n \geq 3$ independent experiments.

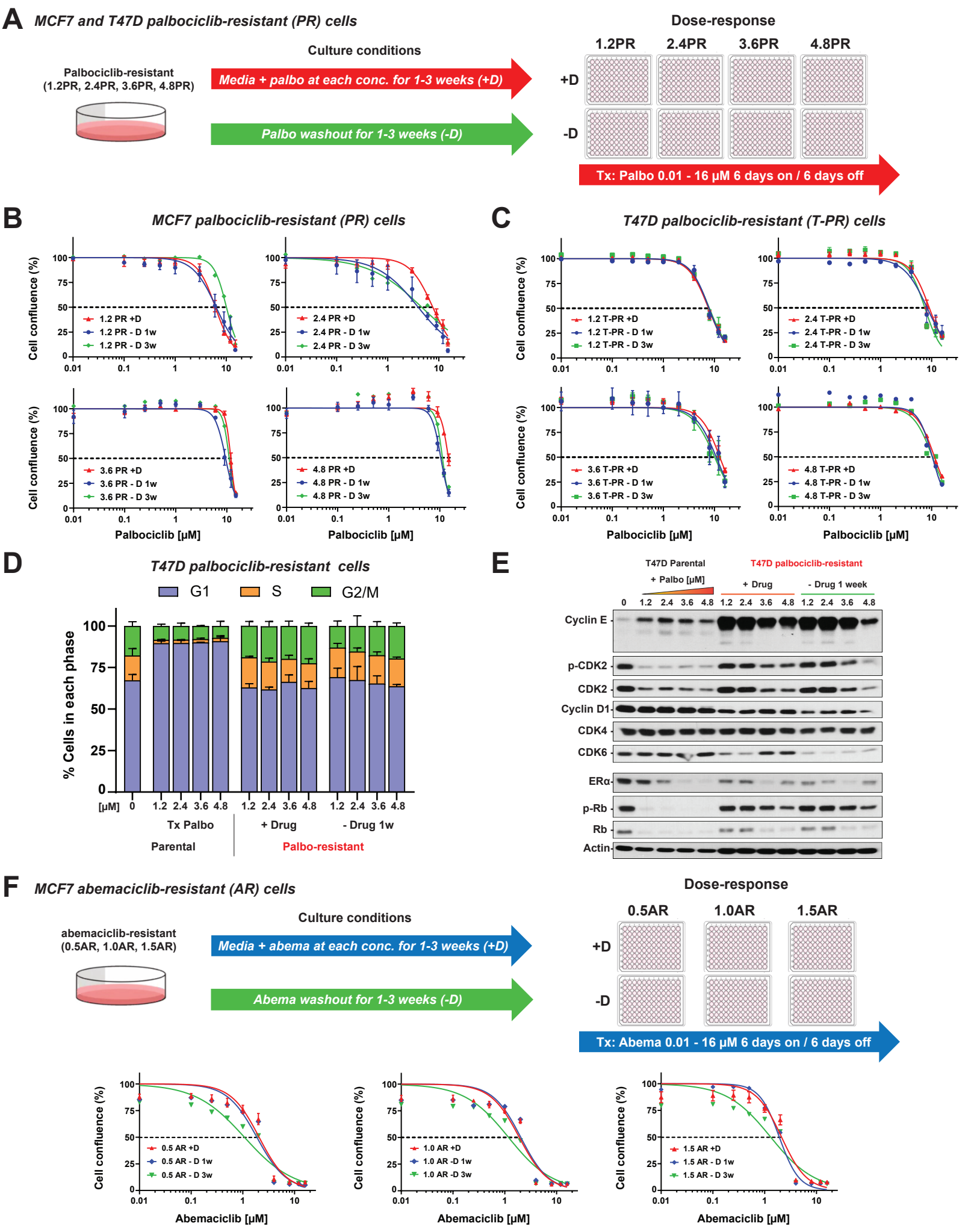

Supplementary Figure 2. Related to Figure 1A - E.

Supplementary Fig. 3. Related to Fig. 1F. A, Volcano plots illustrating the overall distribution of the significant differentially expressed genes (DEGs) from the indicated comparisons. Fold change of genes in different samples is plotted on the x-axes. Statistically significant degree of changes in gene expression levels are plotted on the y-axes; the smaller the corrected *P* value, the bigger the −log10 (adjusted *P* value, *P*-adj) and the more significant the difference. The threshold of DEGs was FDR adj-*P* < 0.05. The dots represent individual genes; black dots indicate genes with no significant difference in expression, red dots indicate upregulated DEGs, and blue dots indicate downregulated DEGs. **B–D**. Principal components analysis (PCA) plots depicting the sample similarity/pattern based on the first two principal components (PCs). The plots show MCF7 parental and the four panels of PR cells **(B)**, T47D parental and the four panels of T-PR cells **(C)**, and MCF7 parental and the three panels of AR cells. **(D)**

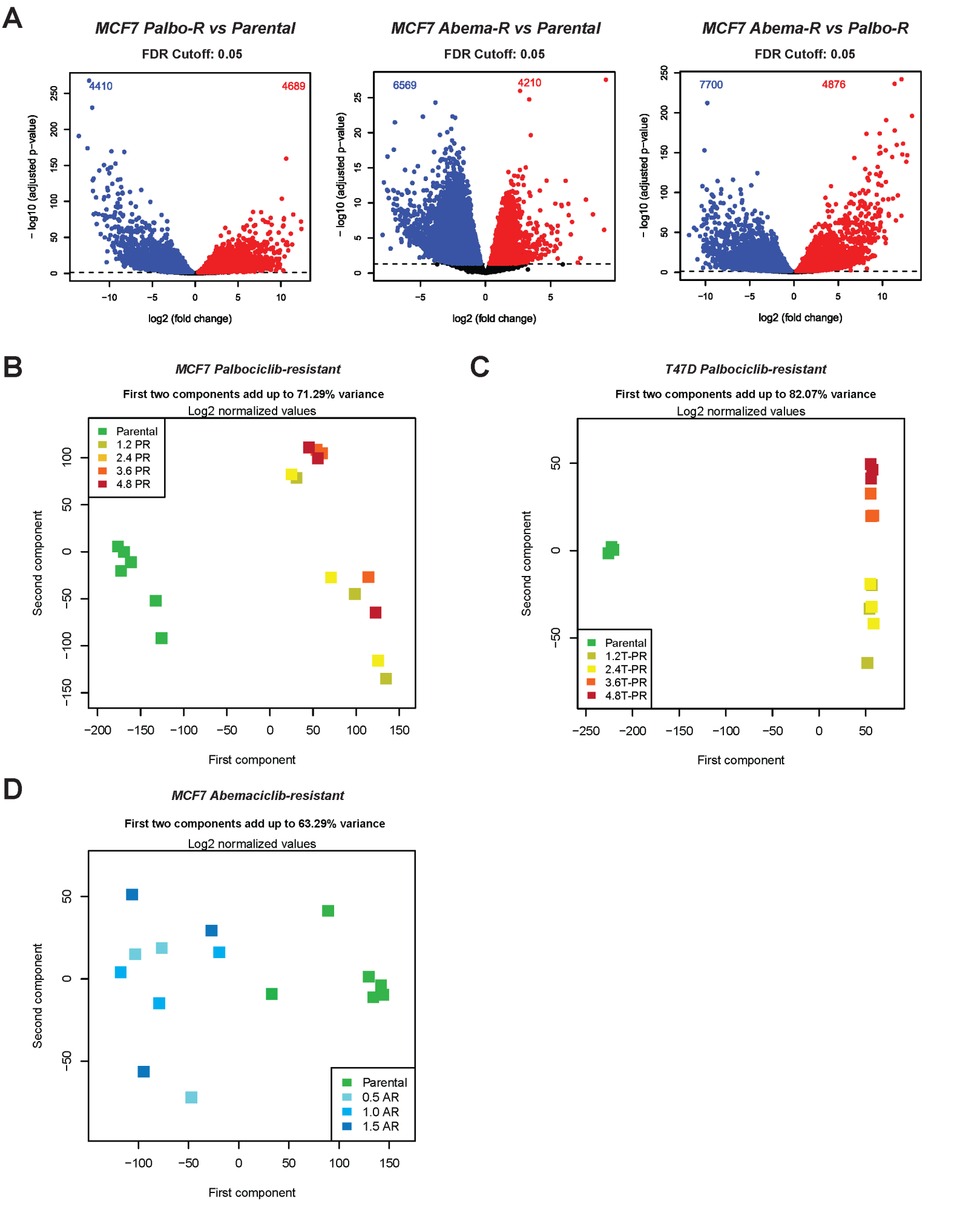

Supplementary Figure 3. Related to Figure 1F

Supplementary Fig. 4. Related to Fig. 1F. Heatmaps of Spearman correlation coefficients between the MCF7 and T47D palbociclib and abemaciclib resistant cells (derived from multiple pools and clones) based on the normalized data. **(A)** Spearman correlation heatmap for palbociclib resistant cells. Samples are ordered by treatment groups. **(B)** Spearman correlation heatmap for abemaciclib resistant cells. Samples are ordered by treatment groups.

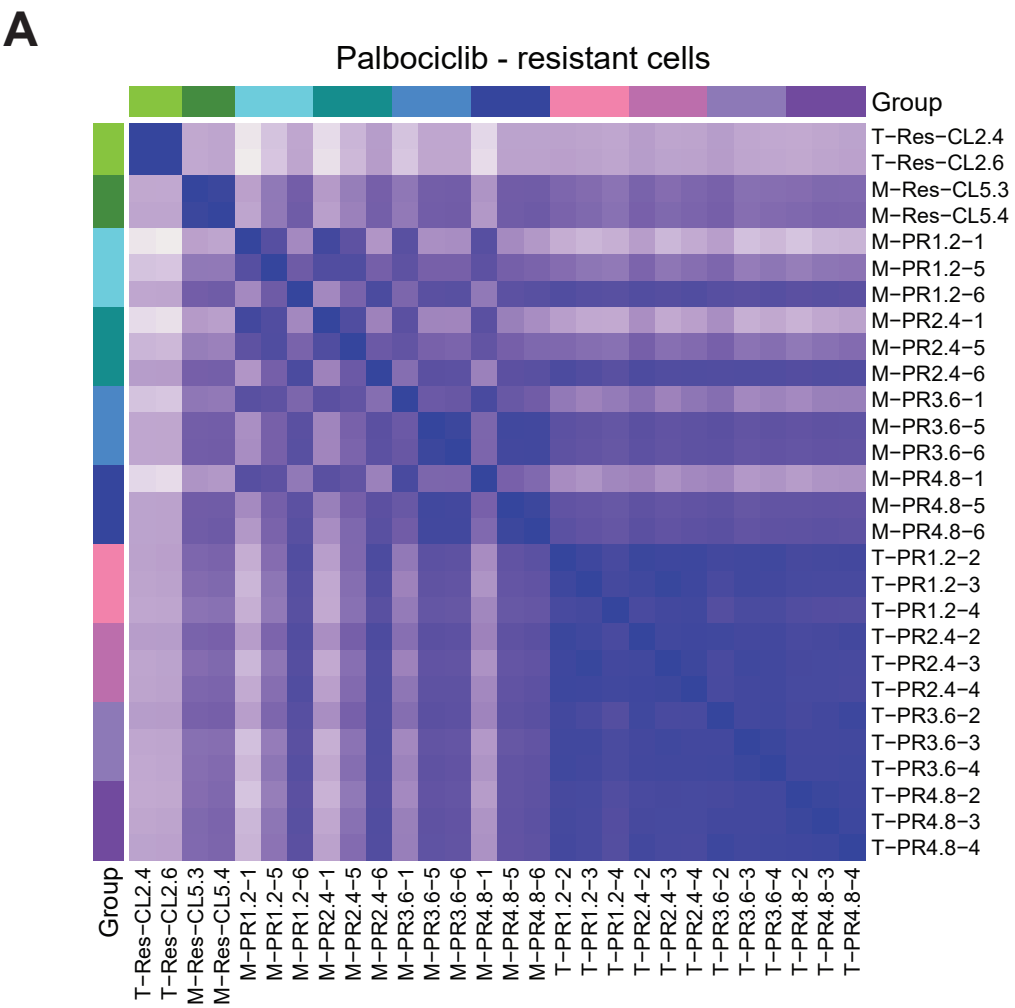

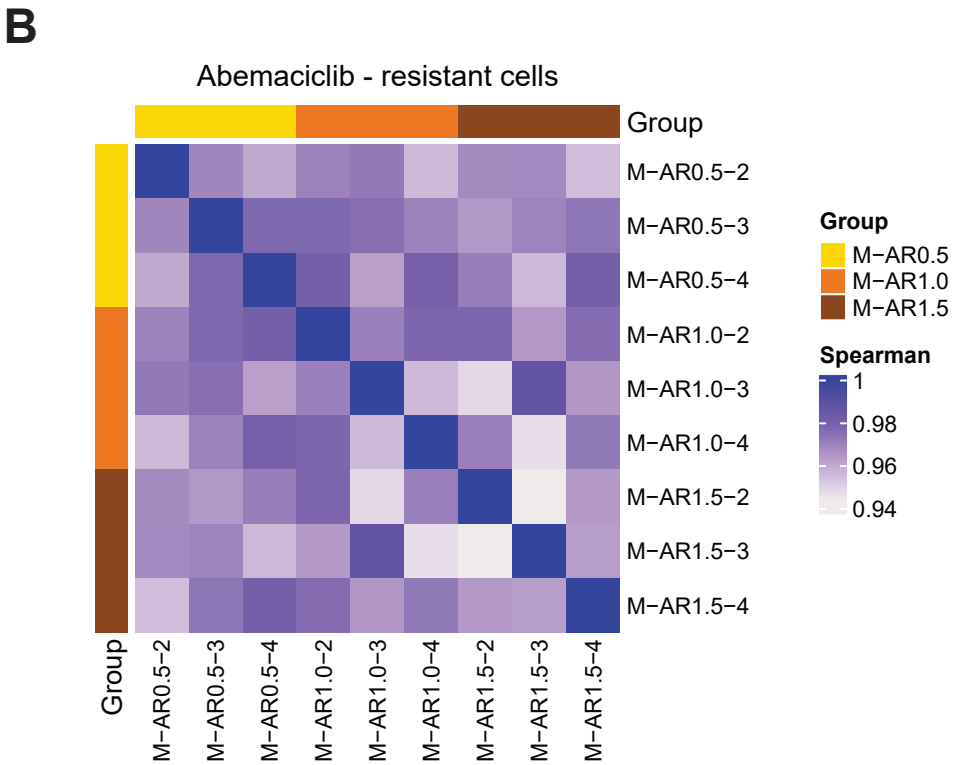

Supplementary Figure 4. Related to Figure 1F

Supplementary Fig. 5. Related to Fig. 1G. GSEA analysis of cancer hallmark pathway gene sets in MCF7 (M) and T47D (T) PR cells. Genes were ranked based on the significance (*P* values) in combination with the sign of log2 fold change values resulting from two-group comparisons (each resistant cell line at each concentration vs parental cells). GSEA was performed for each comparison between resistant cells at each concentration of palbociclib vs parental cells in MCF7 and T47D cells to show how each pathway is enriched between the two cell lines and across each concentration. The color range indicates the normalized enrichment score (NES); the sizes of the dots indicate FDR q-value.

MCF-7 (M) and T47D (T) Palbo-R cells (PR)

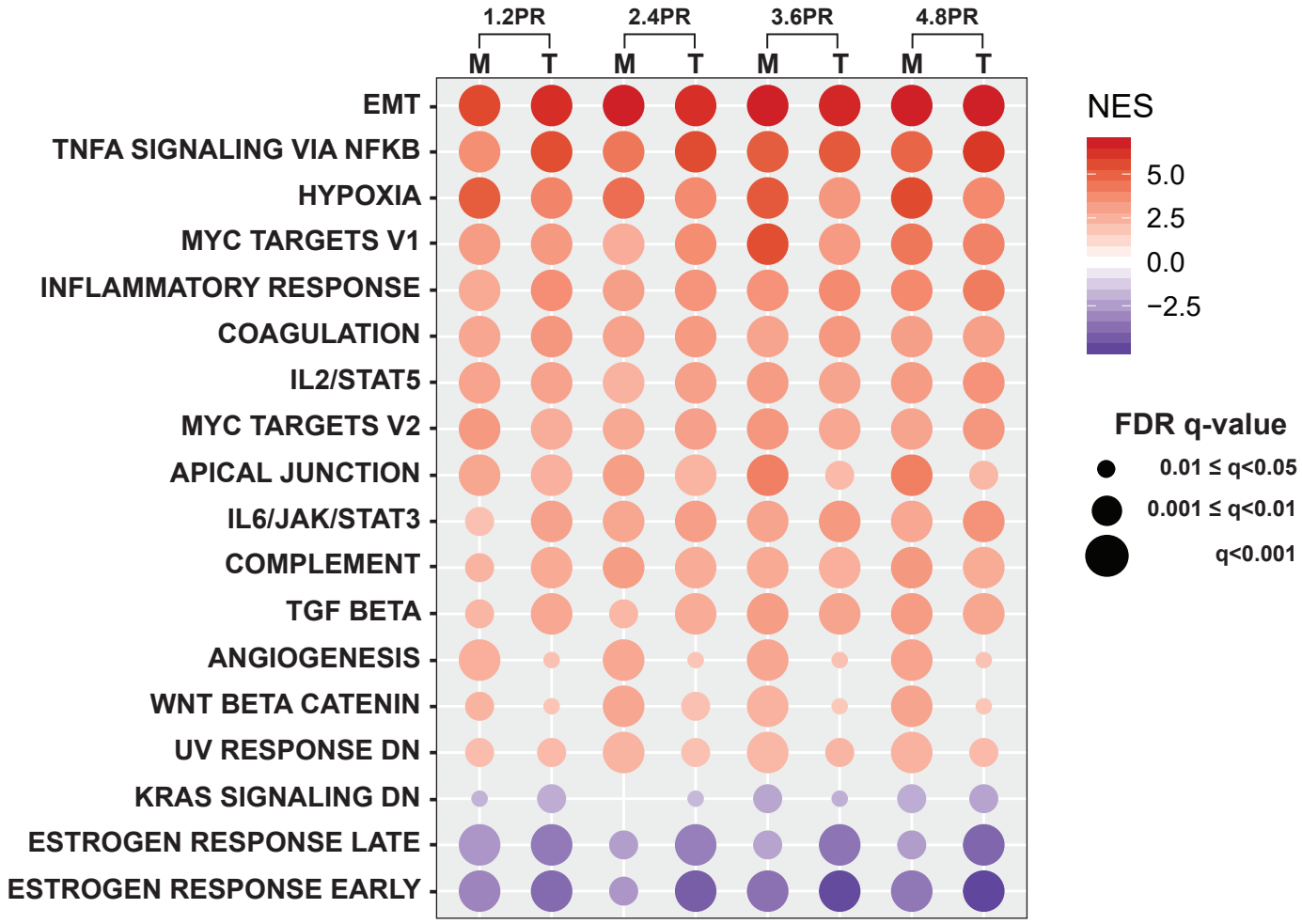

Supplementary Figure 5. Related to Figure 1G

Supplementary Fig. 6. Related to Fig. 2. A, mRNA fold change expression of a chronological EMT signature generated from the literature, assessed in the AR and PR cells relative to parental cells. The color range indicates the magnitude of the fold change; the sizes of the dots indicate the level of statistical significance. **B,** Western blot analysis and validation of EMT markers in MCF7 parental, PR, and AR cells. **C,** Flow cytometry analysis of CD44 and CD24 markers showing the enrichment in cancer stem cell (CSC) population ($CD44^{(+)}$, $CD24^{(-)}$; pink) in parental cells, MCF7 PR cells, MCF7 AR cells, and T47D PR cells. Stacked bars represent the mean percentage of cells ± SEM in each quadrant of the contour plots (as in Fig. 2C); $n \geq 3$ independent experiments. **D,** Levels of secreted IL6, as evaluated by ELISA, in culture media of PR and AR cells. Data represent the mean ± SEM; $n \geq 3$ independent experiments. ** $P = 0.0014$. **E,** Western blot analysis showing the changes in levels of ERα in MCF7 PR cells (left) and MCF7 AR cells (right) compared to parental cells. **F,** Dose-response curves showing the effect of fulvestrant + 10 nM beta-estradiol (E_2) treatment for 72 hours on MCF7 parental, 4.8PR, and AR cells previously deprived of estrogens for 24 hours. Cell confluence/viability was assessed by crystal violet staining. Data were normalized to DMSO (100%), plotted, and analyzed by nonlinear regression using GraphPad Prism 9 software. The dashed line depicts the IC_{50} value for parental cells. IC_{50} values for resistant cells were not reached. Each experiment included eight biological replicates per concentration. Data represent the mean ± SEM; $n = 2$ independent experiments. **G,** Real-time glycolytic rate assay in MCF7 parental, PR, and AR cells. Bars represent the basal rates of glycolysis expressed as the rate of protons extruded into the extracellular medium during glycolysis (glycoPER). The inset graph depicts the kinetic profile of glycolytic proton efflux from live cells into the media. Basal rates were recorded over three measurement periods. Rot and AA, complex I and complex III mitochondrial inhibitors, were injected to inhibit the mitochondrial oxygen consumption (OCR), and the proton efflux rate (PER) from respiration was calculated in order to remove it from the total PER and obtain the glycoPER. A second injection with 2-deoxy-D-glucose (2-DG), a glucose analog that inhibits glycolysis by binding of glucose hexokinase, was

performed to stop glycolytic acidification and confirm pathway specificity. The reduction in PER is a qualitative confirmation that PER produced before the injection was due to glycolysis.

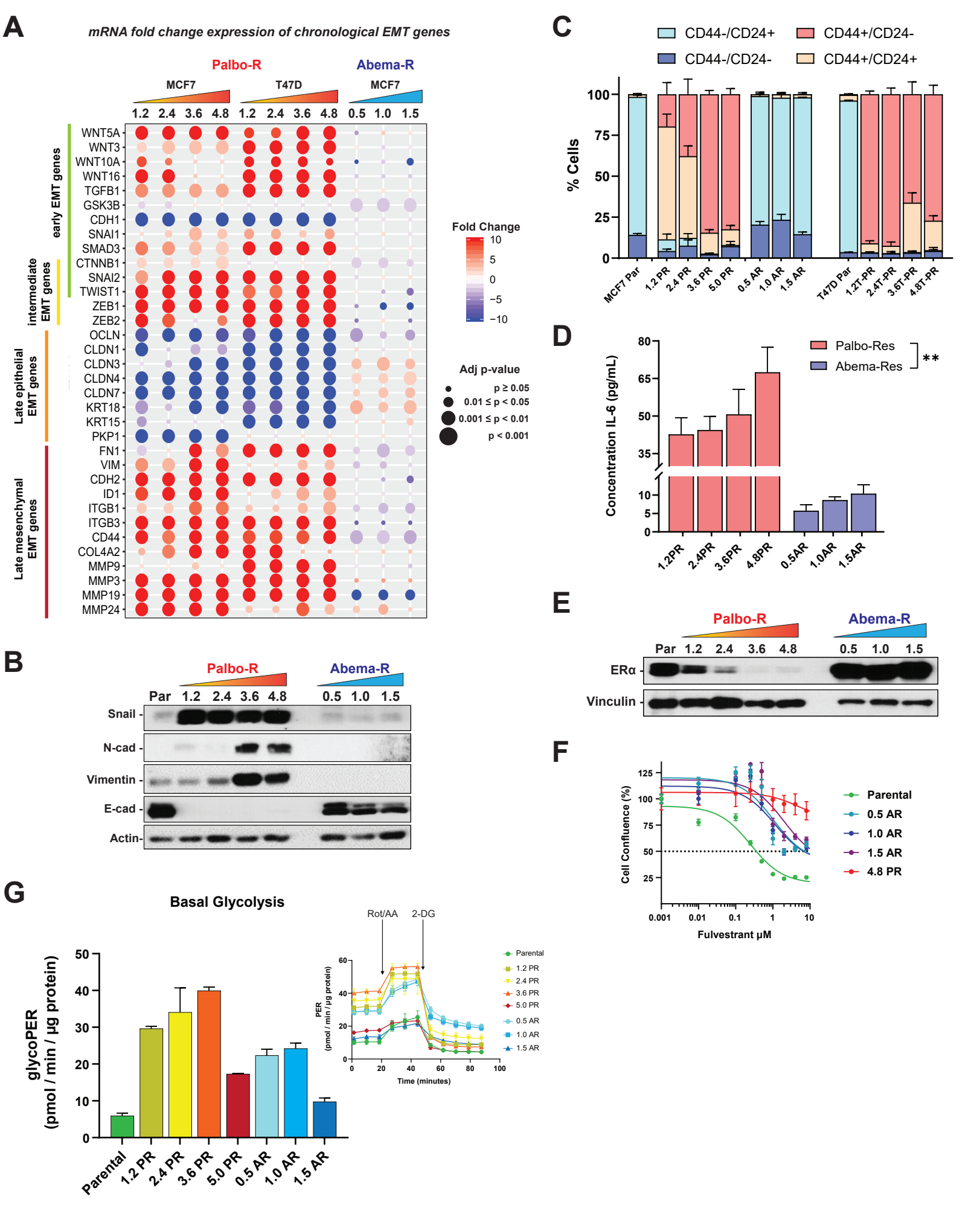

Supplementary Figure 6. Related to Figure 2

Supplementary Fig. 7. Related to Fig. 3D. **(A)** Heat map depicting the IC_{50} values of abemaciclib, palbociclib, and their difference (ΔIC_{50} = IC_{50} palbociclib – IC_{50} abemaciclib) after treatment of MCF7 PR cells with increasing concentrations of palbociclib and abemaciclib (0.01–16 μM) for 6 days, followed by 6 days of recovery in drug–free medium. Data corresponds to Figure 3 and was plotted using GraphPad Prism 9 software**. (B)** Left: Cell cycle analysis in MCF7 parental and 4.8PR cells comparing the effect of treatment with 1 μM abemaciclib for 6 days. Representative histograms of four independent experiments are shown. The percentage of cells in each cell cycle phase is indicated in blue font. Right: Differences between the indicated groups evaluated by two-way ANOVA, Tukey multiple comparisons test. Data represent the mean ± SEM; $n \geq 4$ independent experiments. * $P \leq 0.05$; *** $P \leq 0.001$; **** $P \leq 0.0001$; ns: not significant.

A

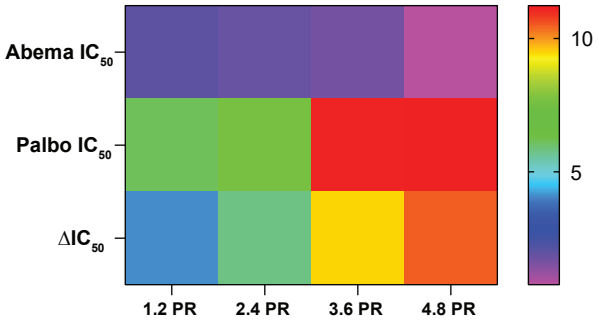

B

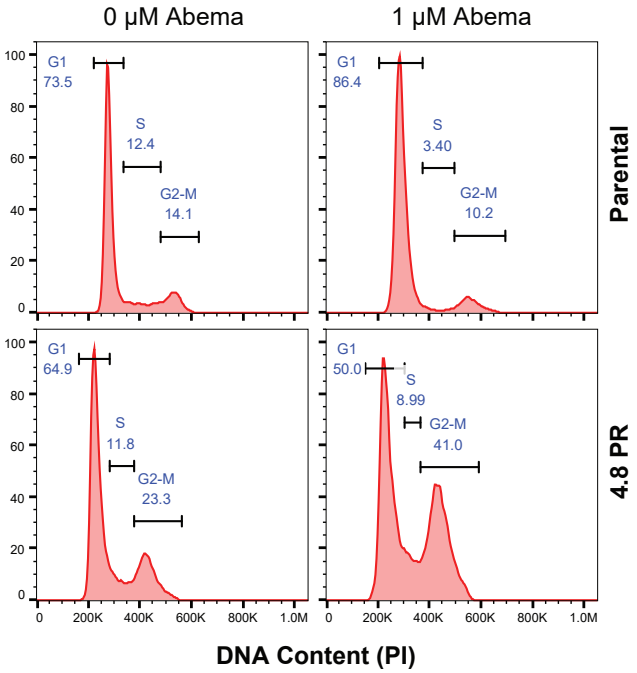

G0/G1	Adj P Value	
Par 0 μM vs. Par 1.0 μM Abe	<0.0001	****
Par 0 μM Abe vs. 4.8PR 0 μM Abe	0.0218	*
Par 1.0 μM Abe vs. 4.8PR 1.0 μM Abe	<0.0001	****
4.8PR 0 μM Abe vs. 4.8PR 1.0 μM Abe	<0.0001	****
S		
Par 0 μM Abe vs. Par 1.0 μM Abe	<0.0001	****
Par 0 μM Abe vs. 4.8PR 0 μM Abe	0.4353	ns
Par 1.0 μM Abe vs. 4.8PR 1.0 μM Abe	0.0005	***
4.8PR 0 μM Abe vs. 4.8PR 1.0 μM Abe	0.9996	ns
G2/M		
Par 0 μM Abe vs. Par 1.0 μM Abe	0.0177	*
Par 0 μM Abe vs. 4.8PR 0 μM Abe	0.0003	***
Par 1.0 μM Abe vs. 4.8PR 1.0 μM Abe	<0.0001	****
4.8PR 0 μM Abe vs. 4.8PR 1.0 μM Abe	<0.0001	****

Supplementary Figure 7. Related to Figure 3

Supplementary Fig. 8. Related to Fig. 4. A, Clinical characteristics of patients whose tumors were used to generate the PDXs and their matched PDxOs. Four different metastatic breast cancer PDX models were established from the liquid nitrogen tumor bank and transplanted into the T4 mammary fat pads of 8-week-old female NSG mice receiving estradiol (E_2; 8 μg/ml)–supplemented drinking water. Tumors were allowed to grow until they reached 1000–1500 mm^3, then were harvested and used for PDX expansion and drug-response studies, as well as organoid (PDxO) generation. **ET-R**, the endocrine therapy–resistant model, was obtained from a patient whose disease progressed during aromatase inhibitor ET and who was CDK4/6i treatment naive. **PR-1 to 4**, palbociclib-resistant (PR) models, were obtained from patients who developed disease progression 3–16 months after starting palbociclib plus ET. **B,** Tumor growth curves illustrating the ET-R PDX model response to abemaciclib (50 mg/kg daily by mouth) and palbociclib (75 mg/kg by mouth, 21 days on/7 days off) treatment. Tumors were allowed to grow until they reached a volume of 100-200 mm^3, in the presence of E_2 (8 μg/mL)–supplemented drinking water. At that point, CDK4/6i treatment was started, and the E_2 supplementation was removed, mimicking the effect of endocrine therapy. The ET-R PDX was shown to be sensitive to both CDK4/6is. The difference between groups was evaluated by one-way ANOVA, Tukey's multiple comparisons test. * $P \leq 0.05$; **** $P \leq 0.0001$. Data represent the tumor volume mean ± SEM; n = 10 mice for vehicle, n = 5 mice for palbociclib, n = 5 mice for abemaciclib. **C,** Hierarchical clustering heatmap depicting the average expression of overlapping G2/M leading-edge genes in MCF7 PR and T47D PR cells. The 57 listed genes constitute the G2/M gene signature. **(D)** Oncoprint for PDX models and MCF7 and T47D cell lines resistant to palbociclib (n=6) on the 34 genes curated from literature associated with potential drivers of resistance to CDK4/6 inhibitors based on the somatic mutation and CNV data. For cell line somatic mutation calling, parental cells were used as a control. Genes are sorted by mutation frequency form high to low. The percentage of samples with any gene alteration is indicated on the right side of the plot. Each column represents a sample. Colors and shapes refer to different variant types. **(E)** Oncoprint for PDX

models and MCF7 and T47D cell lines resistant to palbociclib (n=6) on the 17 genes with mutation in at least two PDX models based on the somatic mutation and CNV data. Genes are sorted by mutation frequency form high to low. The percentage of samples with any gene alteration is indicated on the right side. Each column represents a sample. Colors and shapes refer to different variant types.

A

Patient Characteristics	PDX / PDxO	CDK4/6i response
Stage IV, ER+ / PgR- / HER2- MBC. Aromatase inhibitor-resistant. CDK4/6i naïve.	ET-R	Sensitive
ER+ / PgR+ / HER2- MBC. Disease progression after 16 months on palbociclib + letrozole.	PR-1	Palbo Resistant
ER+ / PgR+ / HER2+ MBC. Disease progression after 6 months on trastuzumab + palbociclib + letrozole.	PR-2	Palbo Resistant
ER+ / PgR+ / HER2- MBC. Disease progression after 3 months on palbociclib + letrozole.	PR-3	Palbo Resistant
ER+ / PgR-/ HER2- MBC. Disease progression after 3 months on palbociclib + fulvestrant.	PR-4	Palbo Resistant

B

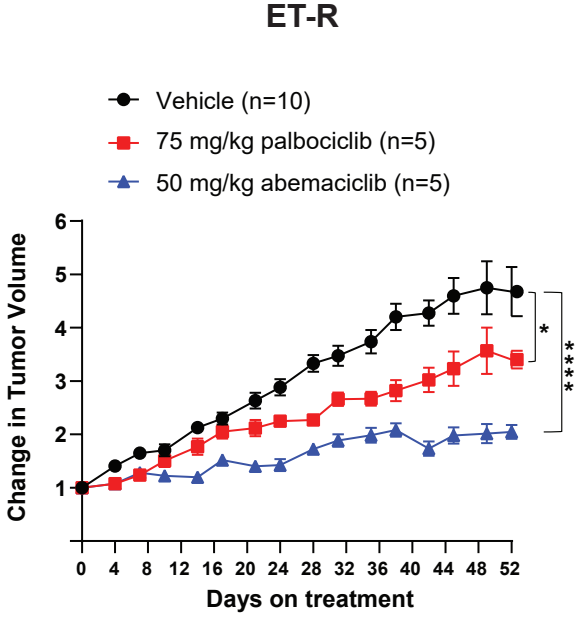

C

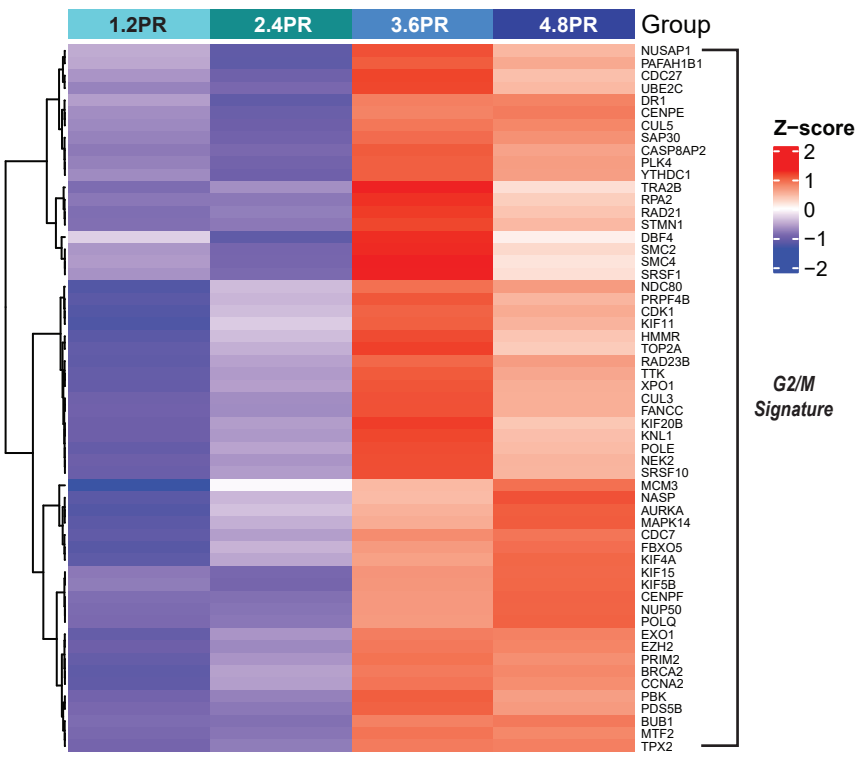

D

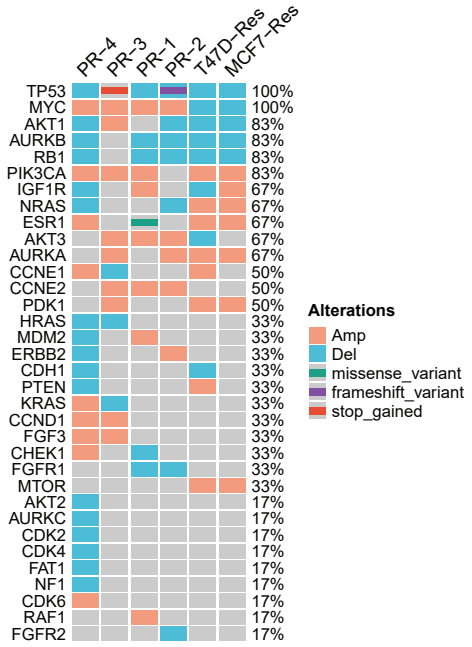

E

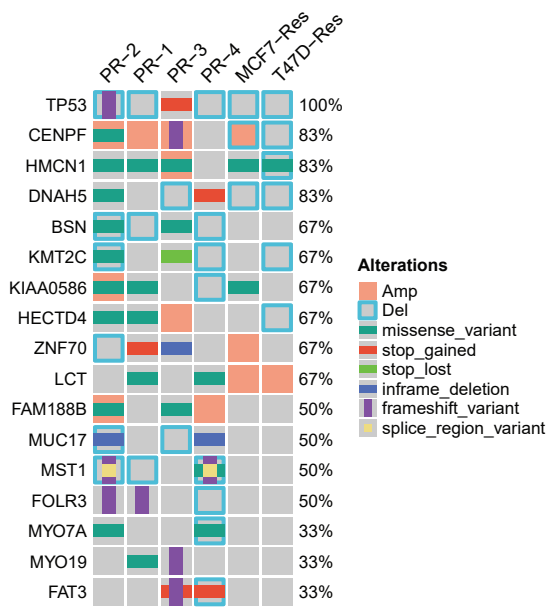

Supplementary Figure 8. Related to Figures 1, 4 and 5

Supplementary Fig. 9. Related to Fig. 5. A, Tumor growth curves of female nude mice bearing the PR-2 PDX model. The curves show the response to abemaciclib (50 mg/kg, by mouth, every day), palbociclib (75 mg/kg, by mouth, 21-day cycle), and vehicle treatment for 36 days. E_2 supplementation was given as described for Supplementary Fig. 7B. The difference between groups was evaluated by two-way ANOVA, Tukey multiple comparisons test. **** $P \leq 0.0001$, ns: not significant. Data represent the tumor volume mean ± SEM for vehicle ($n = 8$), palbociclib ($n = 3$), and abemaciclib ($n = 4$). The length and width of tumor xenografts were measured by calipers 2 or 3 times per week, and the tumor volume was calculated as (length × $(\text{width})^2$)/2. **B,** Survival analysis of female nude mice bearing the PR-2 PDX model and treated as described in **A**. Event-free survival was calculated based on the time on treatment when tumor volume reached 500 mm^3. The difference between survival curves was calculated using the log-rank (Mantel-Cox) test. **C,** Comparison of the response to abemaciclib and palbociclib treatment in the PR-2 PDX model *(in vivo)* and its matched organoids *(ex vivo).* Relative tumor volume (%) was calculated from the experiment shown in **A**, and relative organoid viability (%) was calculated from the experiments shown in Fig. 4E. The difference between groups was evaluated by two-way ANOVA, Tukey's multiple comparisons test. ** $P < 0.01$; *** $P < 0.001$; **** $P < 0.0001$; ns: not significant. **D,** Pearson correlation between the tumor volume and the organoids' viability from experiments shown in **A** and Fig. 4E, respectively. **E,** Gene expression of G2/M and OXPHOS signatures in the PR-3 compared to the PR-4 model. The OXPHOS gene signature used here was derived from the literature, presented in Fig. 2D. The G2/M gene signature is derived from the 57 overlapping gene sets from MCF7 and T47D, presented in Supplementary Fig. 7C.

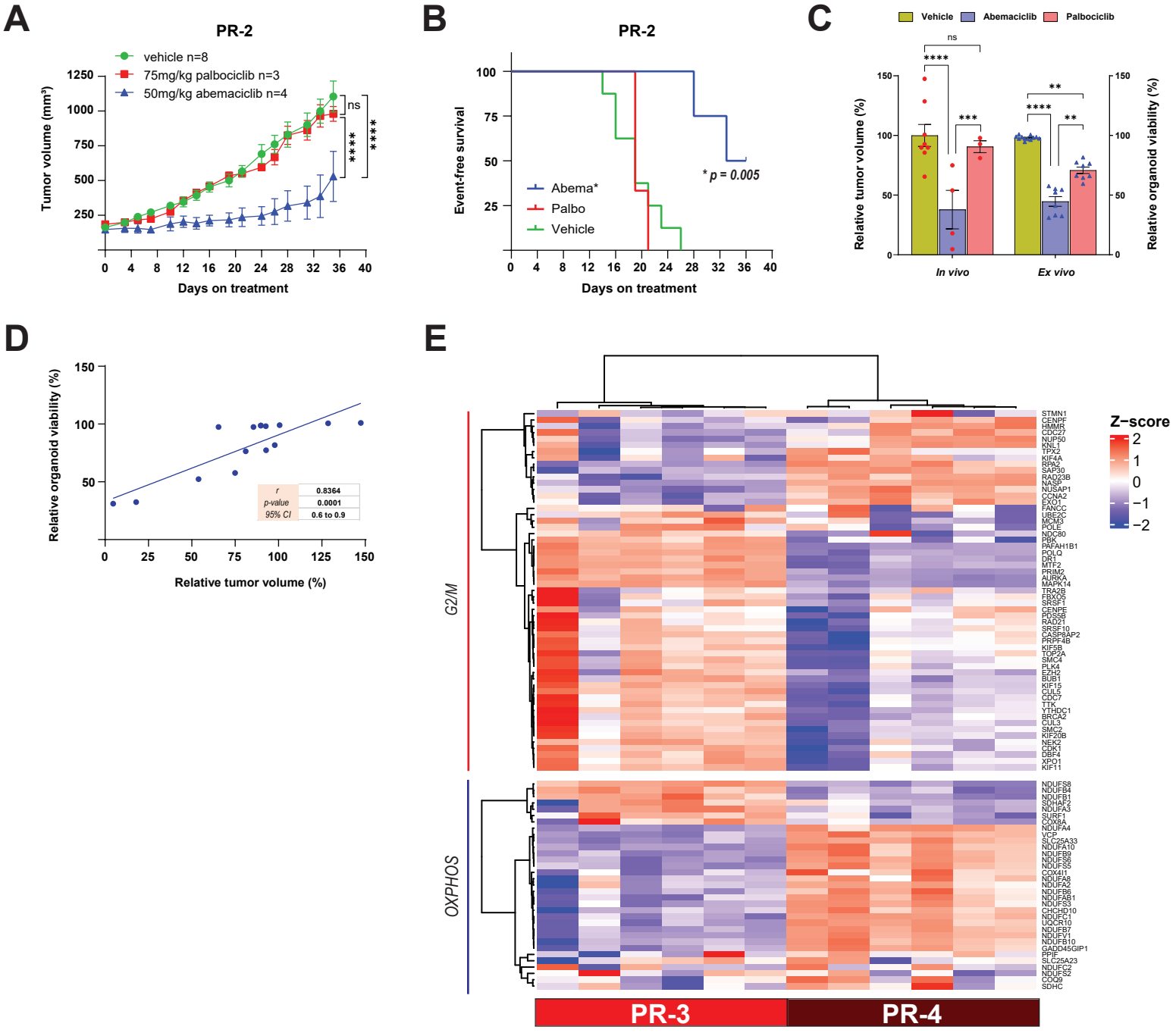

Supplementary Figure 9. Related to Figure 5

Supplementary Fig. 10. Related to Fig. 6. STROBE (Strengthening the Reporting of Observational studies in Epidemiology) diagram depicting the inclusion and exclusion criteria for the patient cohorts used in the retrospective analysis.

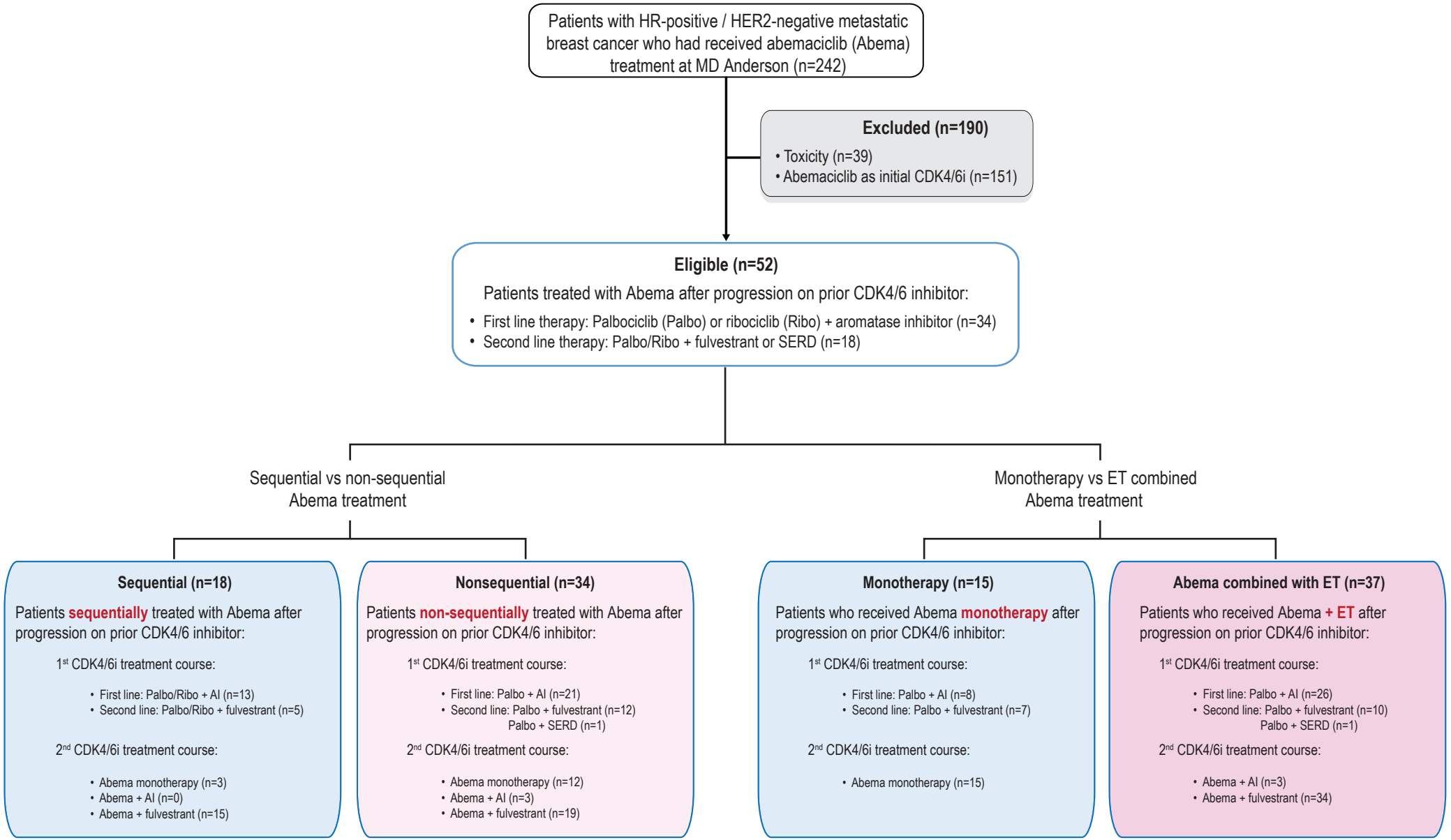

Supplementary Figure 10. Related to Figure 6

Supplementary Figure 11: Distribution of alterations on the gene panel in our dataset of 28 (out of 52) breast cancer patients. Oncoprint plot shows all the genes of interest sorted by mutation frequency from high to low ordered by Sequential and non-Sequential abemaciclib treatment. The percentage of samples with any gene alteration is indicated on the right side. Each column represents a patient sample. Total number of alterations for each sample is indicated in the bar plot on the top. Colors and shapes refer to different variant types.

Supplementary Figure 11. Related to Figure 6

Supplementary Figure 12: Distribution of alterations on the gene panel in our dataset of 28 (out of 52) breast cancer patients. Oncoprint plot shows all the genes of interest sorted by mutation frequency from high to low ordered by events (dead or alive). The percentage of samples with any gene alteration is indicated on the right side. Each column represents a patient sample. Total number of alterations for each sample is indicated in the bar plot on the top. Colors and shapes refer to different variant types.

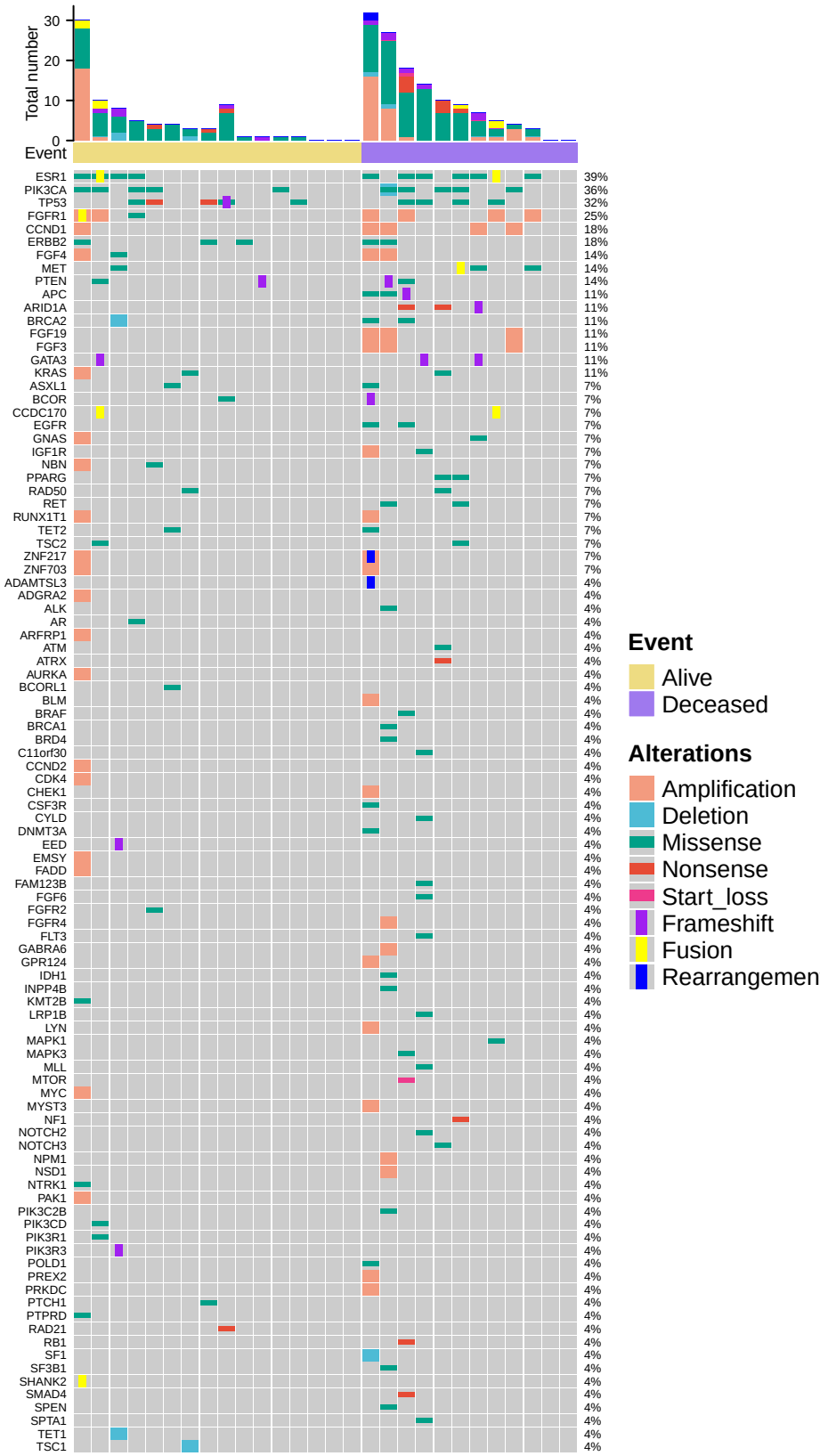

Supplementary Figure 12. Related to Figure 6